JURNAL ILMU KEFARMASIAN INDONESIA
Indonesian Journal of Pharmaceutical Sciences
ISSN p-ISSN 1693-1831 (Print) e-ISSN 2614-6495 (Online) PUBLISHER : Faculty of Pharmacy Universitas Pancasila

Comparative evaluation of magnetic stirrer and homogeniser on globules characterization and stability of red palm oil submicroemulsion prepared by d-phase emulsification method

Elsa Fitria Apriani[1], Tommy Julianto Bustami Effendi[2,3], Windy Keumala Budianti[4], Mahdi Jufri[1]*

[1]*Laboratory of Pharmaceutics and Pharmaceutical Technology, Faculty of Pharmacy, Universitas Indonesia, Depok, 16424, Indonesia*
[2]*Department of Pharmacy, Faculty of Pharmacy, Universiti Teknologi MARA Cawangan Selangor, Puncak Alam Campus, Selangor, 42300, Malaysia*
[3]*Department of Pharmacy Mitra Bunda Health Institute, Batam, 29454, Indonesia*
[4]*Department of Dermatology and Venereology, Faculty of Medicine Universitas Indonesia - Cipto Mangunkusumo National Central General Hospital, Jakarta, 10430, Indonesia*

*Corresponding Author: mahdi.jufri@farmasi.ui.ac.id

Received: 09 January 2026 / Accepted: 23 April 2026

ABSTRACT: Red palm oil (RPO) contains antioxidants due to its carotenoid and vitamin E content. However, the lipophilicity and instability of these two compounds may reduce RPO's bioavailability and efficacy of RPO. This study aimed to develop RPO submicroemulsions and evaluate the effects of magnetic stirrer (M) and homogeniser (H) on their characteristics and physical stability. A submicroemulsion was developed using the D-phase emulsification method. Formulas with globule sizes less than 200 nm, polydispersity index (PDI) less than 0.4, and zeta potential less than -30 mV were tested for stability at room temperature for 3 months and analysed for Ostwald ripening rates. The homogenizer method produced smaller globule sizes and lower PDI ($p<0.05$). Ten formulations from both the magnetic stirrer and homogeniser methods met the initial globule requirements. After 3 months, F4H and F9H showed the best physical stability with globule sizes of 181.23±0.96 and 175.23±1.88 nm, PDI of 0.077±0.034 and 0.035±0.023, and zeta potential of -33.80±0.56 and -30.57±0.15 mV ($p>0.05$). However, F9H had a lower Ostwald ripening rate than F4H, namely 2.54×10^5 and 6.04×10^5 nm^3/month, respectively. In conclusion, the homogeniser produced more stable RPO submicroemulsions than the magnetic stirrer.

KEYWORDS: D-Phase emulsification; physical stability; red palm oil; stirring method; submicroemulsion.

INTRODUCTION

Red palm oil (RPO), extracted from the fruit of the oil palm tree (*Elaeis guineensis* L.), is a natural source of diverse phytonutrients with health benefits. Consequently, RPO holds significant potential as a raw material for nutraceutical, cosmetic, and pharmaceutical applications in the future. Numerous studies have established that red palm oil contains fatty acids (primarily palmitic and oleic acids), carotenoids, vitamin E, phytosterols, squalene, and coenzyme Q10 [1]-[3]. The principal components, carotenoids (notably beta carotene) and vitamin E (in the forms of tocopherol and tocotrienol), are recognized for their potent antioxidant properties [4-6]. These antioxidant properties position RPO as a promising material for the prevention of chronic diseases, including cardiovascular disease, cancer, diabetes, and neurodegenerative disorders, as well as for anti-aging effects and enhanced immune function [7],[8]. However, the high lipophilicity of carotenoids and vitamin E presents challenges in the development of RPO products. Highly lipophilic compounds exhibit low water solubility in the gastrointestinal tract and skin, resulting in poor absorption and low bioavailability [9]. Additionally, lipophilic compounds are more prone to degradation via hydrolysis and oxidation when exposed to oxygen, light, and heat [10]. Therefore, innovative delivery systems are required to protect and improve the absorption of these bioactive compounds.

Submicroemulsions are colloidal dispersion systems consisting of drugs, lipids or oils, surfactants, and hydrophilic cosolvents, and have been demonstrated to be effective delivery systems for lipophilic compounds such as RPO [11]. These systems typically exhibit globule sizes of 100-500 nm [11]. Submicroemulsions have

How to cite this article: Apriani EF, Effendi TJB, Budianti WK, Jufri M. Comparative evaluation of magnetic stirrer and homogeniser on globules characterization and stability of red palm oil submicroemulsion prepared by D-phase emulsification method. Jurnal Ilmu Kefarmasian Indonesia. 2026. 24(1): 81-91.

https://doi.org/10.35814/jifi.v24i1.2042
ISSN: 2614-6495

been extensively studied and have been shown to enhance the kinetic stability and solubility of active compounds and facilitate drug delivery to deeper tissues, making them suitable for oral, topical, and parenteral administration [12]. The small globule size of submicroemulsions increases the surface area, thereby accelerating the dissolution rate and absorption of active compounds in the digestive tract [12]. Furthermore, submicroemulsions can protect active compounds from enzymatic degradation and extreme pH, thereby improving their chemical stability during delivery [12]. Previous studies on drug-loaded submicroemulsions have demonstrated their potency as delivery vehicles. For instance, the transdermal delivery of kaempferol was markedly enhanced when formulated as a submicroemulsion compared to a standard isopropyl myristate control. Specifically, the cumulative amount permeated over 12 h (Q12h) reached 236.1±21.2 µg/cm², a substantial increase from the 4.2±1.8 µg/cm² observed in the control group. Furthermore, these systems significantly shorten the lag time and increase skin deposition [13]. These findings suggest that submicroemulsions can optimize the therapeutic potential of bioactive compounds in RPO.

Submicroemulsions can be prepared using high- or low-energy methods. In high-energy methods, powerful mechanical devices, such as high-pressure homogenizers or ultrasonicators, are used to perform shear and cavitation to reduce the Laplace pressure and break oils into submicron globules [14]. In contrast, low-energy methods do not require such complex devices, significantly reducing production costs and facilitating industrial scale-up in developing countries such as Indonesia [15]. In this study, we used the low-energy D-phase emulsification method. In this method, a D-phase is generated, where some surfactants self-assemble to form a quasi-two-dimensional array (at the oil-water interface of the emulsifying system) to improve the emulsification process. When water is added to the D-phase, the system changes from an oil-in-dispersed (O/D) phase to a submicroemulsion gel. Water and surfactants are known to decrease interfacial tension and increase interfacial flexibility, leading to the formation of submicroemulsions with stable globule sizes (100-200 nm) [16].

The successful formation of stable submicroemulsion globules via the D-phase method is further influenced by the magnitude of the external mechanical energy applied during the transition process. In laboratory and industrial settings, magnetic stirrers and homogenizers are the primary stirring devices employed, although their energy profiles differ considerably. It is important to classify these methods based on the agitation speed and shear intensity. Low-energy agitation, such as conventional magnetic stirring, typically operates at lower speeds (< 3,000 RPM) and focuses on bulk-phase mixing without significant globule fractures. Conversely, high-energy rotor-stator systems operate at significantly higher speeds (typically >3,000 RPM) to generate the localized high-shear intensity required for effective globule breakage [17]. The level of applied shear force directly dictates the submicroemulsion quality, including the globule size, polydispersity index (PDI), and long-term stability. A critical challenge in these nanoscale systems is Ostwald ripening, a destabilization mechanism in which smaller globules dissolve and merge with larger ones owing to differences in the solubility pressure [18]. Although these fundamental mechanisms are well documented, comprehensive studies comparing the deterministic effects of low-speed magnetic stirring with those of high-speed homogenization on the physical stability and kinetic characteristics of RPO submicroemulsions produced using the D-phase method are limited. However, no systematic study has specifically evaluated the comparative effects of magnetic stirring and high-shear homogenization on the physicochemical characteristics and Ostwald ripening behavior of RPO-based submicroemulsions prepared via the D-phase emulsification method.

Based on the background and problems mentioned above, this study aims to compare the effects of two stirring methods, namely the Magnetic Stirrer and homogenizer, during the emulsification process with the D-phase emulsification method in the manufacture of red palm oil submicroemulsions on globule characteristics (globule size, PDI, and zeta potential), long-term stability, and resistance to the Ostwald ripening phenomenon.

MATERIALS AND METHODS

Materials

The materials used in this study were red palm oil (Harvist®), Sucrose Habo Monoester P90 (Compassfood, Singapore), glycerin (Bratachem, Indonesia), and Demineralized Water (Bratachem, Indonesia).

Experimental design

A comparative experimental design was used with the following variables:

1. Independent Variable: The Stirring was applied during the critical D-phase transition stage using two distinct mechanisms:
   - Method M (Magnetic Stirrer): This process was performed using a magnetic stirrer at 1,000 RPM for 30 min with a cylindrical magnetic bar (8 mm × 40 mm) in the transition regime, with a Reynolds number below 3,500.
   - Method H (High-Shear Homogenization): This process was performed using a rotor-stator homogenizer at 1,000 RPM for 15 min **in** transition to a low turbulent Regime with Reynolds number above 3,500.
2. Dependent Variables: Globule size, polydispersity index (PDI), zeta potential, and physical stability
3. Controlled Variable: Composition of the submicroemulsion formula, including RPO, sucrose monoester P90, and glycerin.

Red palm oil submicroemulsion preparation

A red palm oil submicroemulsion was prepared using the D-phase emulsification method [19]. The red palm oil submicroemulsions were prepared in several formulas with red palm oil concentrations ranging from 45-60%, sucrose monoester concentrations ranging from 10-20%, and glycerin concentrations of 30-45%, as shown in Table 1. There were 11 formulas for each stirring method, namely, magnetic stirrer (M) and homogenizer (H).

Table 1. Red palm oil submicroemulsion formula.

Formula	Concentration (%)		
	Red palm oil	Sucrose habo monoester P90	Glycerin
1	52.5	10	37.5
2	47.5	20	32.5
3	45	10	45
4	50	15	35
5	60	10	30
6	47.5	12.5	40
7	50	20	30
8	55	15	30
9	45	17.5	37.5
10	45	25	30
11	52.5	17.5	30

The preparation of red palm oil submicroemulsions involves two main steps: the formation of a submicron-phase gel and the generation of submicroemulsions. Smix was prepared by mixing sucrose habo monoester P90 and glycerin at 80 °C for 5 min until a viscous white mixture was formed. Then, red palm oil preheated at 80 °C for 5 min was added to the Smix and stirred for 5 min. Red palm oil was added dropwise to Smix under continuous stirring using either a magnetic stirrer or homogenizer until a submicron-phase gel was formed. The gel was then dispersed in demineralized water at room temperature and stirred for 1 min to produce a submicroemulsion.

Red palm oil submicroemulsion characterization

Organoleptic

The organoleptic properties of the red palm oil submicroemulsion were assessed based on its shape, color, and odor.

Globule size, polydispersity index (PDI), and zeta potential

The globule size, polydispersity index (PDI), and zeta potential were measured by Dynamic Light Scattering (DLS) using a Particle Size Analyzer. Measurements were performed at 25 °C and a 173° detection angle. The samples were diluted 1:100 with demineralized water. Disposable cuvettes were used for globule size and PDI measurements, and dip-cell cuvettes were used for zeta potential measurements. Each measurement was performed in triplicate [20,21].

Stability assessment of red palm oil submicroemulsion

The stability test was performed at 30±2 °C. The organoleptic properties, globule size, polydispersity index (PDI), and zeta potential were evaluated at 0, 1, 2, and 3 months.

Determination of ostwald ripening rate

Ostwald ripening was assessed by measuring the globule size of the red palm oil submicroemulsion stored at 30±2 °C for three months. The Ostwald ripening rate was calculated using the Lifshitz-Slyozov-Wagner equation as follows [22]:

$r_t{}^3 - r_0{}^3 = \omega \, . \, t$ ..... [Equation 1]

Where:
$r_t{}^3$ = the cubic radius of the oil globules in the submicron emulsion stored for time
$r_0{}^3$ = the cubic radius of the oil globules in the submicron emulsion at day 0
ω = ostwald ripening rate (nm3/months)
t = time (months)

▪ RESULTS

Red palm oil submicroemulsion characterization

The red palm oil submicroemulsions prepared using a magnetic stirrer or homogenizer exhibited organoleptic properties, as shown in Figure 1 and Table 2. As shown in Table 2, the organoleptic evaluation on day 0 showed that all 11 RPO submicroemulsion formulations, regardless of the stirring method (magnetic stirrer or homogenizer), maintained a liquid physical state and were visually homogeneous, with no observed phase separation. The intensity of color (scores 1–3) and odor (scores 2–4) generally correlated with the RPO concentration in each formula. In terms of appearance, although most formulations achieved a transparent state, some formulas processed with the high-speed homogenizer (particularly Formulas 3, 4, 5, and 8) showed an opaque appearance compared to the formulas processed with the magnetic stirrer. This variation suggests that the higher mechanical energy input from the homogenizer in this specific process may have triggered a different globule dispersion pattern and interfacial arrangement.

Figure 1. Organoleptic of red palm oil submicroemulsion from (A) magnetic stirrer, (B) homogeniser

Table 2. Descriptive organoleptic properties of red palm oil submicroemulsions.

Formula	Stirring method	Color intensity	Odor intensity	Shape	Appearance	Stability
1	Magnetic stirrer	1	3	Liquid	Translucent	Homogeneous
	Homogeniser	2	3	Liquid	Translucent	Homogeneous
2	Magnetic stirrer	1	2	Liquid	Translucent	Homogeneous
	Homogeniser	1	2	Liquid	Translucent	Homogeneous
3	Magnetic stirrer	2	2	Liquid	Translucent	Homogeneous
	Homogeniser	3	2	Liquid	Opaque	Homogeneous
4	Magnetic stirrer	3	3	Liquid	Opaque	Homogeneous
	Homogeniser	3	3	Liquid	Opaque	Homogeneous
5	Magnetic stirrer	2	4	Liquid	Translucent	Homogeneous
	Homogeniser	3	4	Liquid	Opaque	Homogeneous
6	Magnetic stirrer	2	2	Liquid	Translucent	Homogeneous
	Homogeniser	2	2	Liquid	Translucent	Homogeneous
7	Magnetic stirrer	1	3	Liquid	Translucent	Homogeneous
	Homogeniser	2	3	Liquid	Translucent	Homogeneous
8	Magnetic stirrer	2	3	Liquid	Translucent	Homogeneous
	Homogeniser	3	3	Liquid	Opaque	Homogeneous
9	Magnetic stirrer	1	2	Liquid	Translucent	Homogeneous
	Homogeniser	2	2	Liquid	Translucent	Homogeneous
10	Magnetic stirrer	1	2	Liquid	Translucent	Homogeneous
	Homogeniser	1	2	Liquid	Translucent	Homogeneous
11	Magnetic stirrer	2	3	Liquid	Translucent	Homogeneous
	Homogeniser	2	3	Liquid	Translucent	Homogeneous

Color Intensity (1: Pale Yellow (Light), 2: Yellow, 3: Deep Yellow, 4: Orange-Yellow, 5: Deep Orange (Dark)) and Odor Intensity (1: No Odor (Neutral), 2: Very Slight RPO Odor, 3: Moderate RPO Odor, 4: Distinctive RPO Odor, 5: Strong/Pungent RPO Odor)

Table 3 summarizes the characteristics of the red palm oil submicroemulsions. Samples prepared with a magnetic stirrer exhibited globule sizes from 183.50 to 436.53 nm, polydispersity index (PDI) values between 0.134 and 0.398, and zeta potentials ranging from -30.03 to -45.63 mV. In comparison, samples prepared with a homogenizer showed globule sizes from 146.27 to 264.57 nm, PDI values between 0.046 and 0.168, and zeta potentials ranging from -33.53 to -46.27 mV. Table 4 presents the results of the statistical analysis.

Table 3. Characteristics of red palm oil submicroemulsions.

Formula	Magnetic stirrer (M)			Homogeniser (H)		
	Globul Size (nm)	PDI	Zeta potential (mV)	Globul size (nm)	PDI	Zeta potential (mV)
1	257.87±2.57	0.255±0.006	-45.63±0.72	222.03±2.17	0.142±0.006	-46.27±0.86
2	299.20±3.63	0.250±0.031	-34.13±0.12	162.27±1.50	0.143±0.001	-33.53±0.76
3	436.53±5.50	0.398±0.027	-30.03±0.65	192.20±0.87	0.116±0.012	-38.27±0.12
4	311.60±4.17	0.276±0.002	-36.70±3.05	160.43±1.40	0.098±0.015	-36.73±0.25
5	282.30±5.93	0.204±0.023	-37.83±0.25	264.57±1.27	0.168±0.032	-40.90±1.81
6	301.70±5.20	0.252±0.002	-34.13±1.10	186.20±3.64	0.073±0.011	-35.47±0.85
7	213.43±1.10	0.164±0.012	-39.00±0.85	190.13±1.81	0.073±0.015	-36.30±0.69
8	303.83±3.76	0.304±0.041	-38.97±1.96	146.27±1.36	0.046±0.013	-34.07±0.55
9	183.50±0.62	0.134±0.017	-37.70±0.82	154.20±1.65	0.064±0.015	-36.33±0.47
10	375.83±4.93	0.239±0.018	-43.97±0.78	165.90±3.64	0.070±0.009	-35.70±0.50
11	312.10±3.76	0.284±0.017	-41.67±0.60	165.03±3.61	0.078±0.010	-36.13±0.65

Table 4. Results of two-way analysis of variance for the effects of formula, preparation method, and interaction on globule characteristics.

Effect	Dependent variables	*p*-value	Partial eta squared
Formula	Globul size	0.000	0.994
	PDI	0.000	0.870
	Zeta potential	0.000	0.934
Preparation Method	Globul size	0.000	0.998
	PDI	0.000	0.964
	Zeta potential	0.001	0.237
Formula * Preparation Method	Globul size	0.000	0.995
	PDI	0.000	0.867
	Zeta potential	0.000	0.852

Two-way ANOVA revealed significant main effects of the Formula and Preparation Method, as well as significant interactions between these factors ($p<0.05$) for all globule parameters. The preparation Method had the greatest impact on globule size (Partial Eta Squared = 0.998), followed by the formula × method interaction (0.995) and the formula factor (0.994). A Partial Eta Squared value near 1.0 indicates that these factors account for most of the variation in globule size. For the polydispersity index (PDI), the Preparation Method was the most influential (Partial Eta Squared = 0.964), while the formula had the largest effect on the zeta potential (Partial Eta Squared = 0.934). These results show that both the formula composition and energy input method are key determinants of globule characteristics.

Stability of red palm oil submicroemulsion

The red palm oil submicroemulsion formula with a globule size of less than 200 nm, PDI of less than 0.3, and zeta potential greater than -30 mV was used for stability testing. Table 5 presents the results of the stability test conducted at room temperature over a three-month period.

Table 5. Stability result.

Formula	Month	Globul size (nm)	PDI	Zeta potential (mV)
9M	0	183.50±0.62	0.134±0.017	-37.70±0.82
	1	240.23±1.32	0.208±0.059	-37.63±0.64
	2	249.00±2.55	0.220±0.022	-33.43±0.59
	3	296.47±6.24	0.243±0.007	-29.93±0.58
2H	0	160.50±0.01	0.139±0.004	-33.53±0.76
	1	163.63±1.20	0.034±0.018	-32.43±1.07
	2	172.40±1.04	0.027±0.018	-31.60±0.35
	3	191.90±0.75	0.177±0.001	-26.40±0.26
3H	0	189.90±3.34	0.071±0.028	-38.27±0.12
	1	196.43±3.69	0.090±0.046	-35.97±0.35
	2	203.23±1.02	0.126±0.019	-24.23±0.32
	3	ND	ND	ND
4H	0	160.37±1.40	0.079±0.018	-36.73±0.25
	1	169.53±1.86	0.043±0.023	-34.57±0.49
	2	175.73±1.14	0.041±0.028	-34.20±0.10
	3	181.23±0.96	0.077±0.034	-33.80±0.56
6H	0	188.23±0.15	0.049±0.033	-35.47±0.85
	1	197.07±2.15	0.067±0.021	-30.87±1.10
	2	ND	ND	ND
	3	ND	ND	ND
7H	0	190.13±1.81	0.073±0.015	-36.30±0.69
	1	190.33±1.30	0.078±0.018	-33.87±0.47
	2	197.87±0.47	0.062±0.017	-26.53±0.85
	3	239.53±3.40	0.198±0.026	-24.63±0.15
8H	0	145.67±1.19	0.055±0.014	-34.07±0.55
	1	166.97±2.35	0.124±0.042	-33.20±0.10
	2	171.87±1.19	0.073±0.027	-31.07±2.30
	3	201.10±2.82	0.224±0.020	-30.87±0.25
9H	0	166.27±1.78	0.037±0.027	-36.33±0.47
	1	171.50±1.78	0.051±0.012	-34.53±0.25

Formula	Month	Globul size (nm)	PDI	Zeta potential (mV)
	2	173.63±0.60	0.063±0.028	-34.03±0.64
	3	175.23±1.88	0.035±0.023	-30.57±0.15
10H	0	167.70±0.56	0.050±0.031	-35.70±0.50
	1	166.87±1.33	0.067±0.012	-31.93±1.01
	2	169.93±1.96	0.055±0.049	-26.27±0.25
	3	173.17±0.95	0.071±0.019	-25.50±0.40
11H	0	162.90±1.60	0.053±0.027	-36.13±0.65
	1	188.17±2.14	0.147±0.023	-32.10±0.44
	2	235.87±27.42	0.198±0.028	-31.77±0.25
	3	240.23±3.71	0.192±0.025	-28.47±0.25

ND = Not Determined

As summarized in Table 5, the stability test conducted at room temperature over a three-month period demonstrated that two formulations (4H and 9H) maintained their integrity and remained within the required specifications throughout the three months, as shown in Figure 2.

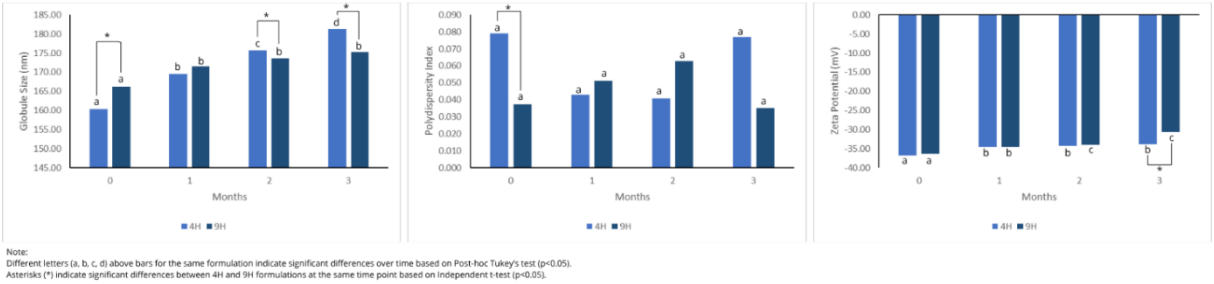

Figure 2. Stability of globule size, PDI, and zeta potential from 4H to 9H.

Ostwald ripening rate of stable formula

The 4H and 9H that were able to maintain the globule characteristic requirements for 3 months of storage were then subjected to the Ostwald ripening rate test. The results of this analysis are shown in Figure 3.

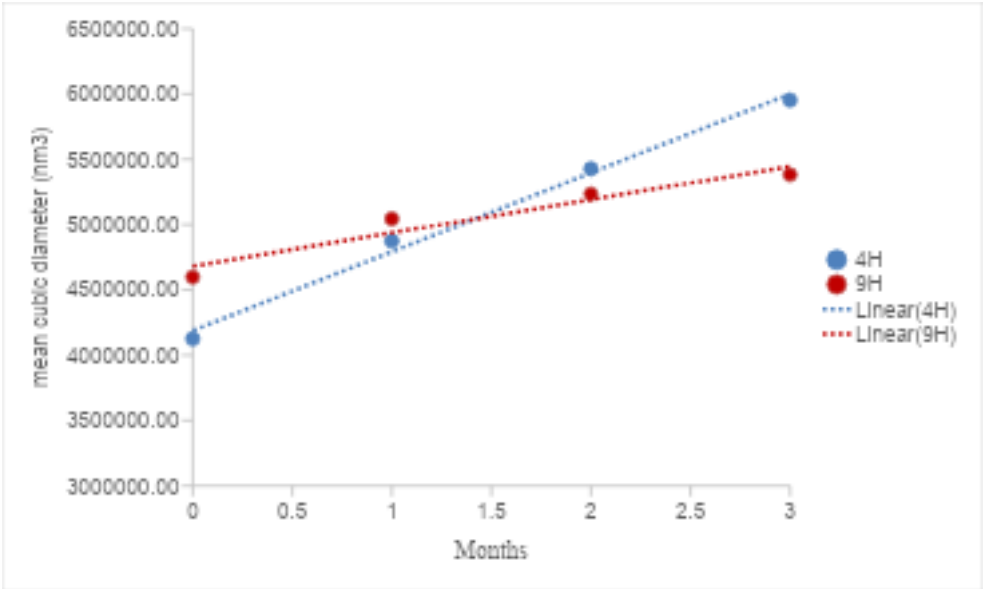

Figure 3. Ostwald ripening rate of 4H and 9H.

▪ DISCUSSION

The homogenizer method was significantly more effective than the magnetic stirrer in producing smaller globule sizes and lower PDI values across most formulations, as shown in Table 3. This disparity in efficiency is fundamentally rooted in the intensity of the mechanical energy and the resulting fluid dynamics. The high-

speed homogenizer generates intense localized shear forces through rapid rotor-stator rotation. This mechanical action creates a high Reynolds Number (Re), often exceeding the threshold for turbulent flow. In this turbulent regime, the system experiences high shear stress and micro-mixing intensity, which are essential for overcoming the Laplace pressure and breaking down the viscous D-phase gel into nanometer-sized globules [23], [24].

In contrast, the magnetic stirrer creates a shear force by rotating a magnetic bar, primarily inducing bulk flow with a significantly lower shear intensity. Although this process produces some turbulence, the energy density is insufficient to achieve the same degree of globule fracture as that of the homogenizer. Consequently, the magnetic stirrer resulted in larger and less uniform globules [25], [26]. Among the formulations tested, F9M emerged as the most successful candidate in the magnetic stirrer group, whereas F9H was identified as the optimal formula overall owing to its superior kinetic stability.

In terms of zeta potential, the magnetic stirrer demonstrated a higher zeta potential than the homogenizer, as shown in Table 3. These contrasting results suggest that the stirring environment influences the differences in surfactant adsorption kinetics on the globule surface. Under the slower and less turbulent shear conditions provided by the magnetic stirrer, surfactant and co-surfactant molecules have more time and a stable environment to migrate and adsorb in a more orderly and dense manner on the surface of the newly formed RPO globules. This organized adsorption leads to the formation of a thicker and more ionized electrical double layer, thereby increasing the absolute zeta potential [27], [28]. In contrast, the high shear energy and intense turbulence generated by the homogenizer may cause partial desorption or disrupt the orientation of the surfactant layer on the globule surface during formation, resulting in a lower zeta potential [29], [30].

The red palm oil submicroemulsion formula with a globule size of less than 200 nm, PDI of less than 0.3, and zeta potential greater than -30 mV was used for stability testing. Various studies have shown that drug particles below 200 nm can increase the solubility and bioavailability of drugs that are difficult to dissolve in water, such as red palm oil [31]. Research conducted by Chono [32] showed that liposomes measuring approximately 200 nm had higher drug delivery efficacy and anti-atherosclerotic effects than those measuring 70 or 500 nm. Jiang et al. [33] also demonstrated that small microparticles (100-200 nm) had higher drug content and retention in tumor tissue than larger microparticles (400-500 nm). In transdermal delivery, particles measuring 200 nm penetrate the stratum corneum into the upper dermis [34]. In this study, a size of 200 nm was set as the size limit that needs to be achieved.

Ten formulations underwent stability testing: one was prepared using a magnetic stirrer and nine using a homogenizer, as shown in Table 5. Formulations F1H and F5H were excluded from further analysis because of their large globule sizes. These findings show that stirring alone does not achieve small globule size. The formation of submicroemulsions requires sufficient mechanical energy and an optimal Smix/oil ratio. Without the right composition, the interfacial tension may not reach the level needed for the high shear energy of the homogenizer to reduce the globule size. F1H and F5H had a Smix:Oil ratio of 1:9. Excessive Smix can lead to micelle or aggregate formation, neutralize the surface charge, reduce electrostatic repulsion, and increase globule size and polydispersity index (PDI) while decreasing zeta potential [35].

Based on the results in Table 5, most formulations did not maintain the expected globule characteristics after the third month. Certain formulations, including F3H and F6H, exhibited phase separation, precluding further globule measurements. These findings indicate that the stability of submicroemulsion formulations is highly dependent on their composition. Only two formulations, F4H and F9H, maintained the desired globule characteristics, with globule sizes of 181.23±0.96 nm and 175.23±1.88 nm, polydispersity index (PDI) values of 0.077±0.034 and 0.035±0.023, and zeta potentials of -33.80±0.56 mV and -30.57±0.15 mV, respectively, at the third month. F4H and F9H had Smix: Oil ratios of 5.67:1 and 4.71:1, respectively. Although F8H and F11H shared similar Smix: Oil ratios with F4H and F9H, the primary difference was the glycerin concentration: F4H and F9H contained more than 35% glycerin, whereas F8H and F11H contained 30%. Increased glycerin concentration enhances the stability of oil-in-water emulsions. Glycerin accumulates at the oil-water interface, resulting in a decrease in interfacial tension [36].

The superior kinetic stability of F9H compared to that of F4H is further explained by the synergistic effect of their specific component concentrations and is confirmed by statistical analysis, as shown in Figure 2. Statistical evaluation using one-way ANOVA followed by Tukey's post-hoc test revealed significant differences in globule size and zeta potential over the three-month storage period for both formulations

(indicated by different letters a, b, c, d above the bars, $p<0.05$). For F4H, a progressive and significant increase in globule size was observed from Month 0 to Month 3 (marked as a–d). In contrast, although F9H also showed an initial increase, it reached a more stable globule after the second month. Furthermore, independent t-tests (indicated by an asterisk *) confirmed that F9H maintained a significantly smaller globule size than F4H at Months 0, 2, and 3 ($p<0.05$).

F9H contained a lower oil volume (45%) than F4H (50%), which inherently reduced the probability of globule collisions and limited the reservoir of oil available for molecular transport during the ripening process. Furthermore, F9H uses a higher concentration of Sucrose Habomonoester P90 (17.5%) than F4H (15%), resulting in denser and more organized surfactant packing at the interface. This dense layer provides a superior steric barrier that prevents the globules from merging. The higher glycerin content in F9H (37.5%) compared to that in F4H (35%) acted as a critical kinetic stabilizer by increasing the viscosity of the continuous phase. According to the LSW theory, this higher viscosity significantly reduces the diffusion coefficient of RPO molecules, thereby inhibiting the Ostwald ripening rate more effectively in the F9H system. The PDI results also showed that F9H initially had a significantly lower and more uniform distribution than F4H ($p<0.05$ at Month 0), which is crucial for preventing early destabilization.

To confirm this mechanism, F4H and F9H were further analyzed to determine their specific Ostwald ripening rates. The results, as illustrated in Figure 3, show that F4H followed the ripening rate equation $y = 603{,}981x + 4{,}188{,}180$ ($R^2 = 0.993$), whereas F9H followed $y = 254{,}398x + 4{,}682{,}454$ ($R^2 = 0.928$). Based on these results, F9H exhibited a significantly lower Ostwald ripening rate than F4H. This enhanced stability in F9H is fundamentally due to the higher glycerin concentration, which facilitates the formation of a thicker oil-water interfacial layer. This thicker layer acts as a more robust mechanical and steric barrier, effectively inhibiting the diffusion of oil molecules out of smaller globules and preventing their incorporation into larger globules [37].

CONCLUSION

The homogenizer-based stirring method outperformed the magnetic stirrer in producing red palm oil submicroemulsions with desirable globule characteristics: globule size below 200 nm, PDI below 0.3, and zeta potential less than -30 mV. Although the absolute zeta potential values were lower than those obtained using the magnetic stirrer, the three-month physical stability test showed that the final stability depended on both the stirring method and formulation composition. Formulas F4H and F9H retained their globule characteristics over three months. Ostwald ripening rate analysis identified F9H as the most stable formula, due to its optimal Smix:Oil ratio of 4.71:1 and high glycerin concentration of 37.5%.

Acknowledgements: The authors thank the Pharmaceutical Technology Laboratory of the University of Indonesia for providing the facilities used in this research.

Funding: This research was funded by the Directorate of Research Funding and Ecosystem, Universitas Indonesia under Hibah PUTI 2025 (Grant No. PKS-57/UN2.RST/HKP.05.00/2025).

Conflict of interest statement: The authors declare no conflicts of interest.

REFERENCES

[1] B. S. R. Zangana and K. O. J. Al-Bahadly, "Estimating of fatty acids, tocopherols, tocotrienols, total carotenes, study the physiochemical properties and unsaponifiable matters extraction from crude RPO," *Baghdad Sci J*, vol. 14, no. 2, pp. 254–261, 2017. doi: 10.21123/bsj.14.2.254-261.

[2] M. Nainggolan and A. G. S. Sinaga, "Characteristics of fatty acid composition and minor constituents of red palm olein and palm kernel oil combination," *J Adv Pharm Technol Res*, vol. 12, no. 1, pp. 22–26, 2021. doi: 10.4103/japtr.JAPTR_91_20.

[3] S. Hidayati, F. Nurainy, E. Suroso, D. Sartika, and S. Hadi, "Effect of heating time on changes in physicochemical properties and fatty acid composition of RPO," *Afr J Food Agric Nutr Dev*, vol. 24, no. 2, pp. 25628–25644, 2024. doi: 10.18697/ajfand.127.23005.

[4] J. Bufka, L. Vaňková, J. Sýkora, and V. Křížková, "Exploring carotenoids: Metabolism, antioxidants, and impacts on human health," *J Funct Foods*, vol. 118, p. 106284, 2024. doi: 10.1016/j.jff.2024.106284.

[5] J. Fiedor and K. Burda, "Potential role of carotenoids as antioxidants in human health and disease," *Nutrients*, vol. 6, pp. 466–488, 2014. doi: 10.3390/nu6020466.

[6] C. C. Chu, S. C. Chew, W. C. Liew, and K. L. Nyam, "Vitamin E: A multi-functional ingredient for health enhancement," *J Food Meas Charact*, vol. 17, pp. 6144–6156, 2023. doi: 10.1007/s11694-023-02042-z.

[7] T. E. Tallei, B. J. Kepel, H. I. S. Wungouw, F. Nurkolis, A. A. Adam, and Fatimawali, "A comprehensive review on the antioxidant activities and health benefits of microgreens: current insights and future perspectives," *International Journal of Food Science and Technology*, vol. 59, no. 1, pp. 58–71, Jan. 2024. doi: 10.1111/ijfs.16805.

[8] A. Muršec, B. Poljšak, A. N. Svete, and V. Erjavec, "Antioxidant strategies for age-related oxidative damage in dogs," *Veterinary Sciences*, vol. 12, no. 10, p. 962, 2025. doi: 10.3390/vetsci12100962.

[9] M. S. Islam and S. Mitra, "Effect of nano graphene oxide (nGO) incorporation on the lipophilicity of hydrophobic drugs," *Hybrid Advances*, vol. 3, p. 100074, 2023. doi: 10.1016/j.hybadv.2023.100074.

[10] Y. Khan *et al.*, "Role of decomposition on drug stability," in *Drug Stability and Chemical Kinetics*, Singapore: Springer Nature, pp. 83-94, 2020. doi: 10.1007/978-981-15-6426-0_7.

[11] V. Mundada, M. Patel, and K. Sawant, "Submicron emulsions and their applications in oral delivery," *Crit Rev Ther Drug Carrier Syst*, vol. 33, no. 3, pp. 265-308, 2016. doi: 10.1615/CritRevTherDrugCarrierSyst.2016017218.

[12] M. Almeida, H. Teixeira, and L. Koester, "Preparation of submicron emulsions: theoretical aspects about the methods employed today," *Latin American Journal of Pharmacy*, vol. 27, pp. 780-788, 2008.

[13] Y. Chao *et al.*, "The effect of submicron emulsion systems on transdermal delivery of kaempferol," *Chem Pharm Bull (Tokyo)*, vol. 60, no. 9, pp. 1171-1175, 2012. doi: 10.1248/cpb.c12-00372.

[14] H. Jasmina *et al.*, "Preparatıon of nanoemulsıons by hıgh-energy and lowenergy emulsıfıcatıon methods," in *Badnjevic, A. (eds) CMBEBIH 2017, IFMBE Proceedings*, Singapore: Springer, 2017. doi:10.1007/978-981-10-4166-2_48

[15] J. S. Komaiko and D. J. McClements, "Formation of food-grade nanoemulsions using low-energy preparation methods: a review of available methods," *Compr Rev Food Sci Food Saf*, vol. 15, no. 2, pp. 331-352, Mar. 2016. doi: 10.1111/1541-4337.12189.

[16] B. Lin *et al.*, "Preparation and mechanism investigation of surfactin-based nanoemulsion by D-phase emulsification," *Colloids and Surfaces A: Physicochemical and Engineering Aspects*, vol. 714, p. 136613, 2025. doi: 10.1016/j.colsurfa.2025.136613.

[17] S. Zhou *et al.*, "Influence of structural parameter variations of high-shear mixers on emulsion particle size," Chemical Engineering Research and Design, vol. 223, pp. 511-523, 2025. doi: 10.1016/j.cherd.2025.10.020

[18] N. Michalak *et al.*, "Ostwald Ripening in an Oxide-on-Metal System," *Advanced Materials Interfaces*, vol. 9, no. 17, p. 2200222, 2022. doi: 10.1002/admi.202200222.

[19] M. N. Yukuyama *et al.*, "High internal vegetable oil nanoemulsion: D-phase emulsification as a unique low energy process," *Colloids and Surfaces A: Physicochemical and Engineering Aspects*, vol. 554, pp. 296–305, 2018. doi: 10.1016/j.colsurfa.2018.06.023.

[20] Miksusanti, E. F. Apriani, and A. H. B. Bihurinin, "Optimization of tween 80 and PEG-400 Concentration in Indonesian virgin coconut oil nanoemulsion as antibacterial against *Staphylococcus aureus*," *Sains Malaysiana*, vol. 52, no. 4, pp. 1259–72, Apr. 2023.

[21] E. F. Apriani, M. Mardiyanto, and A. Hendrawan, "optimization of green synthesis of silver nanoparticles from *Areca catechu* L. seed extract with variations of silver nitrate and extract concentrations using simplex lattice design method," *Farmacia*, vol. 70, no. 5, pp. 917–24, 2022.

[22] W. Park, J. Park, S. Im, and S. J. Choi, "Influence of the type and concentration of hydrocolloids on Ostwald ripening of emulsions stabilized with small molecular and non-ionic surfactants," *Food Chem*, vol. 411, p. 135504, 2023.

[23] J. Fukutomi *et al.*, "Study of Emulsification Mechanism in a Pressure Type Homogeniser," *TRANSACTIONS OF THE JAPAN SOCIETY OF MECHANICAL ENGINEERS Series B*, vol. 79, no. 806, pp. 2030-2040, 2013. doi: 10.1299/kikaib.79.2030.

[24] T. Sumitomo *et al.*, "Study of internal flow and emulsification effect in a homogeniser (Fluids Engineering)," *Transactions of the Japan Society of Mechanical Engineers Series B*, vol. 75, no. 759, pp. 2199-2206, 2009. doi: 10.1299/kikaib.75.759_2199.

[25] E. Sokolov, D. Kalyuzhnaya, and P. Ryapolov, "Behavior of "Non-magnetic liquid-magnetic fluid" emulsions in microchannels under the influence of an inhomogeneous magnetic field," *IEEE Transactions on Magnetics*, vol. 61, no. 9, pp. 1-5, Sept. 2025. Art no. 9200705. doi: 10.1109/TMAG.2025.3544657.

[26] N. T. Nguyen, S. H. Tan, and J. Liu, "Magnetically mediated formation of ferrofluid emulsion," in *ASME 2011 9th International Conference on Nanochannels, Microchannels, and Minichannels, ICNMM 2011*, vol. 2, 2011. doi: 10.1115/ICNMM2011-58212.

[27] E. M. Uhlig and A. S. Khair, "Double-layer structure and interfacial tension at an ionic surfactant-laden interface," *Journal of Colloid and Interface Science*, vol. 697, p. 137924, 2025. doi: 10.1016/j.jcis.2025.137924.

[28] A. A. Shahir, A. V. Nguyen, and S. I. Karakashev, "A quantification of immersion of the adsorbed ionic surfactants at liquid|fluid interfaces," *Colloids and Surfaces A: Physicochemical and Engineering Aspects*, vol. 509, pp. 279-292, 2016. doi: 10.1016/j.colsurfa.2016.08.082.

[29] Y. Shen and H. Hoffmann, "formation of unique unilamellar vesicles from multilamellar vesicles under high-pressure shear flow," *J Phys Chem B*, vol. 122, no. 37, pp. 8706-8711, Sep. 2018. doi: 10.1021/acs.jpcb.8b04646.

[30] L. Zhou *et al.*, "Effects of high-speed shear homogenization on the emulsifying and structural properties of myofibrillar protein under low-fat conditions," *J Sci Food Agric*, vol. 99, no. 14, pp. 6500-6508, Nov. 2019. doi: 10.1002/jsfa.9929.

[31] T. Lorenz and A. Dietzel, "Microfluidic 3D flow-focusing for precipitation and concentration of drug nanoparticles," in *MikroSystemTechnik Kongress 2017 "MEMS, Mikroelektronik, Systeme", Proceedings*, pp. 238-241, 2017.

[32] S. Chono, "Development of drug delivery systems for targeting to macrophages," *Yakugaku Zasshi*, vol. 127, no. 9, pp. 1419–1430, 2007. doi: 10.1248/yakushi.127.1419.

[33] Z. Jiang *et al.*, "Small tumour microparticle enhances drug delivery efficiency and therapeutic antitumour efficacy," *Cancer Nano*, vol. 13, p. 19, 2022. doi: 10.1186/s12645-022-00125-y.

[34] R. Su *et al.*, "Size-dependent penetration of nanoemulsions into epidermis and hair follicles: implications for transdermal delivery and immunization," *Oncotarget*, vol. 8, no. 24, pp. 38214-38226, Jun. 2017. doi: 10.18632/oncotarget.17130.

[35] S. Daware, V. Raje, A. Patel, and K. Patel, "Investigating key molecular descriptors affecting particle size: a predictive exemplary approach for self-emulsifying system," *Molecular Pharmaceutics*, vol. 20, no. 5, pp. 2556-2567, 2023. doi: 10.1021/acs.molpharmaceut.2c01118.

[36] Q. Zhang *et al.*, "Effect of oil structure on adsorption behavior of emulsifier at the oil-polyol interface and the emulsion features," *Colloids and Surfaces A: Physicochemical and Engineering Aspects*, vol. 703, p. 135198, 2024. doi: 10.1016/j.colsurfa.2024.135198.

[37] R. Zhao *et al.*, "Cutoff ostwald ripening stability of eugenol-in-water emulsion by co-stabilization method and antibacterial activity evaluation," *Food Hydrocolloids*, vol. 107, p. 105925, 2020. doi: 10.1016/j.foodhyd.2020.105925.